

Characterization of Five- and Six-Coordinate Iron(III) Complexes of *N*-Methylporphyrins

Alan L. Balch,^{*,†} Charles R. Cornman,[†] Lechosław Latos-Grażyński,[†] and Marilyn M. Olmstead[†]

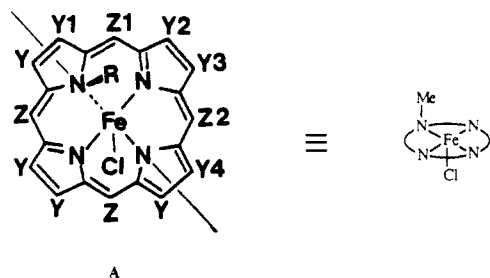
Contribution from the Departments of Chemistry, The University of California, Davis, California 95616, and The University of Wrocław, Wrocław, Poland.
Received November 20, 1989. Revised Manuscript Received May 1, 1990

Abstract: The coordination chemistry of iron(III) in the environment of *N*-methylporphyrins has been expanded to include a crystallographic characterization of a high-spin, five-coordinate complex, [*N*-methyltetra-*p*-tolylporphyrinFe^{III}Cl]·[SbCl₆]⁻·1.5(toluene), which crystallizes in the triclinic space group *P* $\bar{1}$ with *a* = 13.170 (6) Å, *b* = 14.591 (1) Å, *c* = 15.702 (14) Å, α = 83.78 (7)°, β = 79.82 (6)°, γ = 74.34° at 130 K, refined to *R* = 0.069 for 4842 data and 375 parameters, and spectroscopic (¹H and ²H NMR) characterization of low-spin (*S* = 1/2) six-coordinate forms with two strong-field axial ligands (cyanide, imidazole, or substituted imidazole). Thus the steric effects of *N*-methyl substitution *do not* preclude the addition of axial ligands on the same side of the porphyrin plane, but planar ligands like imidazole lie with their planes perpendicular to the C_s plane of the complex. Rotation about the Fe–N imidazole bond on the same side of the plane as the porphyrin *N*-methyl group is restricted, and as a consequence all pyrrole protons of the *N*-methylated porphyrin are nonequivalent. Titration of [(*N*-MeTTP)Fe^{III}Cl][SbCl₆]⁻ with cyanide proceeds through the formation of high-spin [(*N*-MeTTP)Fe^{III}CN][SbCl₆]⁻, with the cyanide bound on the opposite face from the *N*-methyl substituent, and a second, low-spin species which must have the cyanide ligand bound on the same side as the *N*-methyl substituent and either a chloride or no ligand in the other axial site. *N*-Methylporphyrins are readily prepared in 90% yield through the use of methylidiphenylsulfonium tetrafluoroborate, and this has allowed the preparation of the sterically encumbered *N*-methyltetramesitylporphyrin for the first time. The thianthrene cation radical proves to be an excellent oxidant for the preparation of iron(III) complexes of *N*-methylporphyrins.

Introduction

The study of *N*-alkylporphyrins^{1,2} has recently become focused on their biological formation and its implications. *N*-substituted porphyrins are formed during the operation of cytochrome P-450 and by the reaction of substituted hydrazines with heme proteins. Their formation results in the inactivation of the proteins involved.^{2,3} *N*-substituted porphyrins are inhibitors of ferrochelatase and heme oxygenase.¹

The presence of the *N*-methyl substituent lowers the symmetry of the porphyrin core to C_s (see structure A) and renders the two faces of the core inequivalent. Because the *N*-methyl substituent is positioned near the center of the porphyrin, it presents a serious steric barrier that plays a role in governing metal ion coordination. The coordination chemistry of *N*-substituted porphyrin complexes of iron has largely focused on the iron(II) complexes, (*N*-MeP)Fe^{II}Cl, structure A, which are surprisingly stable to aerial oxidation.⁴ These high-spin (*S* = 2) species have roughly



square-pyramidal geometry with the axial chloride coordinated to the face of the porphyrin that is distal to the *N*-methyl substituent.^{4,5} The electronic absorption spectra⁴ and ¹H NMR spectral characteristics⁶ of these compounds have also been thoroughly examined. Other divalent transition-metal ions (Mn(II), Co(II), Ni(II), Zn(II)) are also found to be stabilized in a five-coordinate complex, (*N*-MeP)M^{II}Cl, with the M–Cl bond

distal to the *N*-Me substituent,^{1,4} and generally it has been assumed that the *N*-methyl group precludes coordination to the proximal face.^{1,4}

The oxidation of the iron(II) complexes to iron(III) species, [(*N*-MeP)Fe^{III}Cl]⁺, has been studied both electrochemically^{4,7} and chemically.⁸ The iron(III) complex, [(*N*-MeOEP)Fe^{III}Cl]⁺, has been isolated by Ogoshi and co-workers as the FeCl₄⁻ and ClO₄⁻ salts from the reaction of *N*-MeOEPH with iron(II) chloride and an unidentified oxidant.⁹ The reaction of (*N*-MeTPP)Fe^{II}Cl with silver perchlorate yields the μ -oxo complex [(*N*-MeTPP)Fe^{III}OFe^{III}(*N*-MeTPP)]²⁺,¹⁰ an antiferromagnetically-coupled compound. The related [(*N*-MeTPP)Fe^{III}OFe^{III}(TPP)]⁺ has been thoroughly characterized and shown to be bridged through the unhindered face to the *N*-methylporphyrin.^{10,11} Oxidation of (*N*-MeTTP)Fe^{II}Cl with halogens (chlorine, bromine, or iodine) in chloroform at –50 °C gave high-spin (*S* = 5/2) [(*N*-MeTTP)Fe^{III}Cl]⁺. The cation was characterized in solution by spectroscopic means but it underwent demetalation (when chlorine was used as the oxidant) or demethylation (when bromine was the oxidant) when the solution was warmed. This work established that the iron(III) *N*-methylporphyrin complexes were very sensitive to the chemical environment in which they are formed. Here we describe further studies of the coordination chemistry of these species that has been facilitated by both the adaption of an im-

(1) Lavallee, D. K. *The Chemistry and Biochemistry of N-Substituted Porphyrins*; VCH Publishers: New York, 1987.

(2) Ortiz de Montellano, P. R.; Reich, N. O. In *Cytochrome P-450, Structure, Mechanism and Biochemistry*; Ortiz de Montellano, P. R., Ed.; Plenum Press: New York, 1986; p 273.

(3) Ortiz de Montellano, Correia, M. A. *Annu. Rev. Pharmacol. Toxicol.* **1983**, *23*, 481.

(4) Anderson, O. A.; Kopelove, A. B.; Lavallee, D. K. *Inorg. Chem.* **1980**, *19*, 2101.

(5) Balch, A. L.; Chan, Y. W.; Olmstead, M. M.; Renner, M. W. *J. Org. Chem.* **1986**, *51*, 4651.

(6) Balch, A. L.; Chan, Y. W.; La Mar, G. N.; Latos-Grażyński, L.; Renner, M. W. *Inorg. Chem.* **1985**, *24*, 1437.

(7) Lançon, D.; Cocolios, P.; Guillard, R.; Kadish, K. M. *J. Am. Chem. Soc.* **1984**, *106*, 4472.

(8) Balch, A. L.; La Mar, G. N.; Latos-Grażyński, L.; Renner, M. W. *Inorg. Chem.* **1985**, *24*, 2432.

(9) Ogoshi, H.; Kitamura, S.; Toi, H.; Aoyama, Y. *Chem. Lett.* **1982**, 495.

(10) Wyslouch, A.; Latos-Grażyński, L.; Grzeszczuk, M.; Drabent, K.; Bartczak, T. *J. Chem. Soc., Chem. Commun.* **1988**, 1377.

(11) Bartczak, T.; Latos-Grażyński, L.; Wyslouch, A. *Inorg. Chim. Acta*. Submitted for publication.

[†] University of California, Davis.

[†] University of Wrocław.

[‡] Abbreviations: P, porphyrin dianion; *N*-MeP, *N*-methylporphyrin monoanion; TTP, tetra-*p*-tolylporphyrin dianion; *N*-MeTTP, *N*-methyltetra-*p*-tolylporphyrin monoanion; *N*-MeTTP, *N*-methyltetra-*p*-tolylporphyrin monoanion; *N*-MeTMP, *N*-methyltetramesitylporphyrin monoanion; Thian⁺, thianthrene radical cation.

proved method of synthesis of *N*-methylporphyrins and a procedure of forming the iron(III) complexes with a nonreactive counterion. This work demonstrates that it is possible for ligands to bind to iron on either face of an *N*-methylporphyrin complex.

Results and Discussion

Synthesis of *N*-Methylporphyrins. Conventional syntheses of *N*-methylporphyrins involve treating the porphyrin with one of a variety of alkylating agents: methyl iodide, dimethyl sulfate, methyl fluorosulfate, or methyl trifluoromethanesulfonate.¹ Typically the yields from these procedures are less than 35%. The success of Lavalley, Mansuy, and co-workers¹² in using benzyl-diphenylsulfonium salts as benzylating agents for porphyrins suggested that the use of methyl-diphenylsulfonium salts would improve the routes to *N*-methylporphyrins and indeed it does. When tetraarylporphyrins are treated with methyl-diphenylsulfonium tetrafluoroborate at 140 °C (the optimal temperature) in *o*-dichlorobenzene, the corresponding *N*-methylporphyrin is formed and may be isolated in 90% yield. We have found that the methyl-diphenylsulfonium tetrafluoroborate is made most rapidly and conveniently by the reaction of methyl iodide, diphenyl sulfide and silver tetrafluoroborate¹³ rather than the procedure involving anisole, diphenyl sulfate and an acid.¹⁴ This porphyrin alkylation procedure works for a variety of tetraarylporphyrins. In the Experimental Section, we describe, in detail, the preparation of the sterically encumbered *N*-methyltetramesitylporphyrin, which has been obtained in 90% yield through this route. Previous attempts in this laboratory to obtain this substance through the use of methyl iodide, dimethyl sulfate, or methyltrifluoromethylsulfonate as alkylating agents were unsuccessful.

Oxidation of $(N\text{-MeP})\text{Fe}^{\text{II}}\text{Cl}$ to High-Spin, Five-Coordinate $[(N\text{-MeP})\text{Fe}^{\text{III}}\text{Cl}]^+$. As part of a program to investigate the higher oxidation states available to iron within the *N*-methylporphyrin environment, we examined the reactivity of $(N\text{-MeTTP})\text{Fe}^{\text{II}}\text{Cl}$ with the thianthrene cation radical. This species is known to oxidize iron(III) porphyrin complexes, e.g. $(\text{TTP})\text{Fe}^{\text{III}}\text{Cl}$, to iron(III) complexes of porphyrin π radicals, e.g. $[(\text{TPP}^+)\text{Fe}^{\text{III}}\text{Cl}]^+$.¹⁵ Treatment of $N\text{-MeTTPFe}^{\text{II}}\text{Cl}$ with $(\text{Thian}^+)\text{SbCl}_6$ in dichloromethane yields a brown solution from which $[(N\text{-MeTTPFe}^{\text{III}}\text{Cl})][\text{SbCl}_6]$ may be obtained by evaporation. Recrystallization from toluene/hexane gives a crystalline product suitable for analysis by X-ray diffraction. Other tetraarylporphyrin complexes including $N\text{-MeTMPFe}^{\text{II}}\text{Cl}$ undergo one-electron oxidations. The reactions are readily monitored by ¹H NMR and UV-vis spectroscopy and the spectral patterns observed are entirely consistent with those seen for the related iron(III) complexes formed by oxidation by molecular halogens.⁸ Addition of further quantities of $(\text{Thian}^+)\text{SbCl}_6$ does not alter the NMR spectra. Thus further oxidation above the level of $[(N\text{-MeTTP})\text{Fe}^{\text{III}}\text{Cl}]^+$ is not possible with this oxidant. However, the oxidation with $(\text{Thian}^+)\text{SbCl}_6$ has the distinct advantage of forming samples of $[(N\text{-MeP})\text{Fe}^{\text{III}}\text{Cl}]^+$ that are stable to demetalation or demethylation.

The Crystal Structure of $[(N\text{-MeTTP})\text{Fe}^{\text{III}}\text{Cl}][\text{SbCl}_6] \cdot 1.5(\text{toluene})$. The structure of $[(N\text{-MeTTP})\text{Fe}^{\text{III}}\text{Cl}][\text{SbCl}_6] \cdot 1.5(\text{toluene})$ has been determined by X-ray crystallography. The asymmetric unit consists of the cation, two half ions of SbCl_6^- situated at centers of symmetry, a molecule of toluene that is disordered into two slightly rotated forms in which the methyl carbons could not be found, and a half molecule of toluene that was positioned in disordered fashion about a center of symmetry. These units are well separated in the crystal with no unusual contacts between them.

The structure of cation is shown in Figure 1. Selected interatomic distances and angles are given in Table I where they are compared to those of $(N\text{-MeTTP})\text{Fe}^{\text{II}}\text{Cl}$.⁴ In both, the iron

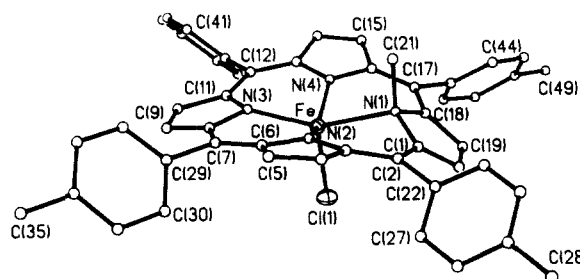


Figure 1. A perspective view of the cation of $[(N\text{-MeTTP})\text{Fe}^{\text{III}}\text{Cl}][\text{SbCl}_6]$ showing 50% thermal contours for Fe and Cl and uniform, arbitrarily sized circles for other atoms.

Table I. Comparison of Selected Parameters in Fe^{III} and Fe^{II} *N*-Methyltetraphenylporphyrin Complexes

	$[(N\text{-MeTTP})\text{Fe}^{\text{III}}\text{Cl}][\text{SbCl}_6]$	$(N\text{-MeTTP})\text{Fe}^{\text{II}}\text{Cl}$
Distances (Å)		
Fe-N(1)	2.259 (8)	2.329 (2)
Fe-N(2)	2.045 (7)	2.118 (2)
Fe-N(3)	2.004 (9)	2.082 (2)
Fe-N(4)	2.050 (8)	2.116 (2)
Fe-Cl	2.164 (3)	2.244 (1)
Fe-N ₃	0.57	0.62
N(1)-C(21)	1.537 (14)	1.511 (3)
Angles (deg)		
N(1)-Fe-Cl	98.6 (1)	103.5 (1)
N(2)-Fe-Cl	104.4 (3)	105.4 (1)
N(3)-Fe-Cl	108.9 (3)	114.4 (1)
N(4)-Fe-Cl	107.7 (2)	108.1 (1)
N(1)-Fe-N(2)	83.8 (3)	82.2 (2)
N(2)-Fe-N(3)	88.8 (3)	87.1 (2)
N(3)-Fe-N(4)	88.2 (3)	86.6 (2)
N(4)-Fe-N(1)	83.8 (3)	82.3 (2)
N(1)-Fe-N(3)	152.5 (3)	142.1 (2)
N(2)-Fe-N(4)	147.0 (3)	145.6 (2)
Fe-N(1)-C(21)	102.0 (6)	98.0 (2)

^aDistance from iron to the plane of N(2), N(3), and N(4).

has approximate square-pyramidal geometry with the chloride ligand lying at the unique apex. The *N*-methyl substituent lies on the face opposite the chloride and the iron is asymmetrically disposed within the porphyrin macrocycle. It has a short bond (2.004 (9) Å) to N(3), the nitrogen trans to the methylated nitrogen, slightly longer bonds (2.045 (7), 2.050 (9) Å) to N(2) and N(3), and a much longer bond (2.259 (8) Å) to N(1). For comparison, in $(\text{TTP})\text{Fe}^{\text{III}}\text{Cl}$ the four Fe-N distances are equal (2.049 (9) Å)¹⁶ and comparable to the Fe-N distances in the *N*-methyl cation except for the one involving N(1), the methylated nitrogen. Likewise, the Fe^{III} -Cl distance (2.164 (3) Å) in the cation is similar to that in $(\text{TPP})\text{Fe}^{\text{III}}\text{Cl}$ (2.192 (12) Å).¹⁶ As expected all bond distances in the Fe^{III} cation are shorter than those found in the Fe^{II} complex, $(N\text{-MeTTP})\text{Fe}^{\text{II}}\text{Cl}$,⁴ as seen in Table I. The pattern of Fe-N distances, however, remains the same. On average the Fe-ligand distances contract by 0.073 Å with the Fe-Cl distance decreasing by the largest amount (0.080 Å) and the Fe-N(4) distance by the least (0.066 Å). As a result of this contraction, the iron is drawn into the plane of the three normal nitrogens N(2), N(3), and N(4). The iron is displaced 0.57 Å out of that plane toward the axial chloride in $[(N\text{-MeTTP})\text{Fe}^{\text{III}}\text{Cl}]^+$ while it is 0.62 Å out of the similar plane in $(N\text{-MeTTP})\text{Fe}^{\text{II}}\text{Cl}$ and 0.38 Å from the N₄ plane in $(\text{TPP})\text{Fe}^{\text{III}}\text{Cl}$.

The macrocyclic core in $[(N\text{-MeTTP})\text{Fe}^{\text{III}}\text{Cl}]^+$ is far from planar. While the three pyrrole rings containing N(2), N(3), and N(4) reside close to a common plane, the methylated pyrrole is sharply tipped out of that plane. This is the pattern seen for other *N*-alkylated porphyrin complexes.^{4,5} However, the direction of the tipping of the pyrrole plane opposite to the *N*-methyl group

(12) Lavalley, D. K.; White, A.; Diaz, A.; Battioni, J.-P.; Mansuy, D. *Tetrahedron Lett.* **1986**, *27*, 3521.

(13) Trost, B. M.; Bogdanowicz, M. J. *J. Am. Chem. Soc.* **1973**, *95*, 5298.

(14) Badet, B.; Julia, M. *Tetrahedron Lett.* **1979**, 1101.

(15) Gano, P.; Buissons, G.; Duée, E.; Marchon, J.-C.; Erlor, B. S.; Scholz, W. F.; Reed, C. A. *J. Am. Chem. Soc.* **1986**, *108*, 1223.

(16) Hoard, J. L.; Cohen, G. H.; Glick, M. D. *J. Am. Chem. Soc.* **1967**, *89*, 1992.

Table II. Chemical Shifts (ppm) for *N*-Methylporphyrin Compounds

compound	pyr	pyr	pyr	pyr	<i>N</i> -CH ₃	temp, K	solvent	ref
(<i>N</i> -MeTTP)Fe ^{III} (CN) ₂	-56.9	-34.2	-31.5	0.0	-61	183	CD ₂ Cl ₂	this work
[(<i>N</i> -MeTTP)Fe ^{III} (5-MeIm) ₂] ²⁺	-38.8	-25.5	-11.1	<i>b</i>		183	CD ₂ Cl ₂	this work
		-24.4	-10.2					
[(<i>N</i> -CD ₃ TTP- <i>d</i> ₃)Fe ^{III} (5-MeIm) ₂] ²⁺	-38.4 ^a	-24.7 ^a	-10.6 ^a	-0.3 ^a	-17 ^a	183	CH ₂ Cl ₂	this work
[(<i>N</i> -CD ₃ TTP)Fe ^{III} (5-MeIm) ₂] ²⁺					-17 ^a	183	CH ₂ Cl ₂	this work
[(<i>N</i> -MeTTP)Fe ^{III} Im ₂] ²⁺	-46.1	-36.3	-18.7	<i>b</i>	-30	183	CD ₂ Cl ₂	this work
	-41.5	-29.7	-15.8					
[(<i>N</i> -MeTTP)Fe ^{III} Cl] ⁺	128	92	79	2	272 ^c	223	CDCl ₃	8
[(<i>N</i> -MeTTP)Fe ^{III} O] ₂ ²⁺	14.7	13.9	12.4	6	6	303	CDCl ₃	10
[(<i>N</i> -MeTTP)Fe ^{III} OFe ^{III} (TTP)] ⁺	14.4	13.8	12.1	6	6	303	CDCl ₃	10
(<i>N</i> -MeTTP)Fe ^{II} Cl	41.9	31.7	-0.3	-0.4	105.0	29.6	CDCl ₃	6
(<i>N</i> -MeTTP)Ni ^{II} Cl	92.6	68.2	33.7	-7.8	177.8	213	CDCl ₃	21
(<i>N</i> -MeTTP)Co ^{II} Cl	61.2	58.3	55.1	-5.8	-104.1	213	CDCl ₃	<i>d</i>

^a²H NMR. ^b Not observed, presumably in diamagnetic region. ^c²H NMR on *N*-CD₃ species; see ref 8. ^dLatos-Grażyński, L. *Inorg. Chem.* **1985**, *24*, 1104.

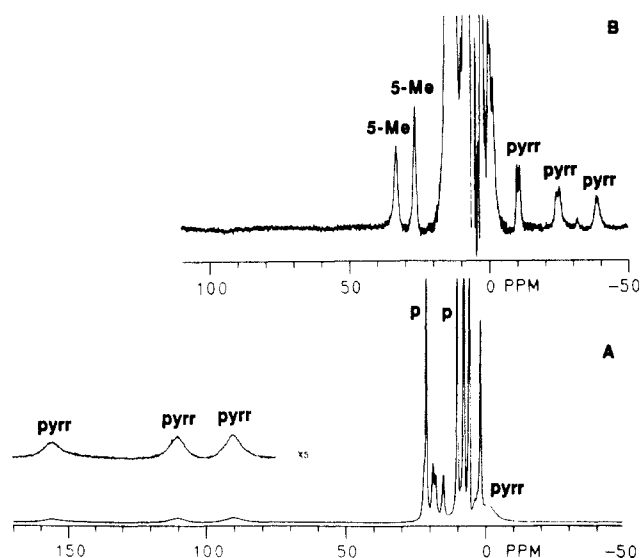
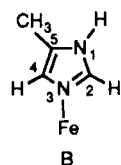


Figure 2. 300-MHz ¹H NMR spectra of (A) [(*N*-MeTTP)Fe^{III}Cl]-[SbCl₆], (B) [(*N*-MeTTP)Fe^{III}Cl][SbCl₆] and 13 equiv of 4-methylimidazole in dichloromethane-*d*₂ at -90 °C. Resonance assignments are pyrr (pyrrole), p (para methyl of tolyl groups), m (meta tolyl protons), and 5-Me (methyl protons of coordinated 5-methylimidazole).

is the reverse of that seen for the iron(II) form. Thus deviations of the pyrrole planes from the plane defined by N(2)-N(3)-N(4) are as follows: N(1) +39.0°, N(2) -14.5°, N(3) +6.8°, N(4) -12.2° for [(*N*-MeTTP)Fe^{III}Cl]⁺ and N(1) +36.6°, N(2) -9.8°, N(3) -6.4°, N(4) -11.3° for (*N*-MeTTP)Fe^{II}Cl.¹

Formation of Low-Spin, Six-Coordinate Complexes by Addition of Bases to [(*N*-MeTTP)Fe^{III}Cl]⁺. Addition of an excess of base (cyanide ion, imidazole, or substituted imidazole) to a solution of [(*N*-MeTTP)Fe^{III}Cl]⁺ or [(*N*-MeTTP)Fe^{III}Cl]⁺ in dichloromethane at low temperature results in their conversion to six-coordinate, low-spin complexes.

The effect of adding 4-methylimidazole (which coordinates as 5-methylimidazole (structure B) to avoid steric interaction with the porphyrin plane) to [(*N*-MeTTP)Fe^{III}Cl]⁺ is shown in Figure 2. Trace A shows the spectrum of the original iron(III) complex



in dichloromethane at -90 °C while trace B shows the sample after the addition of 13 equiv of 4-methylimidazole. Addition of the 4-methylimidazole results in the loss of resonances due to the high-spin iron(III) complexes and the formation of a new set of resonances that may be identified as resulting from [(*N*-MeTTP)Fe^{III}(5-MeIm)₂]²⁺. Comparison of the ²H NMR spectra

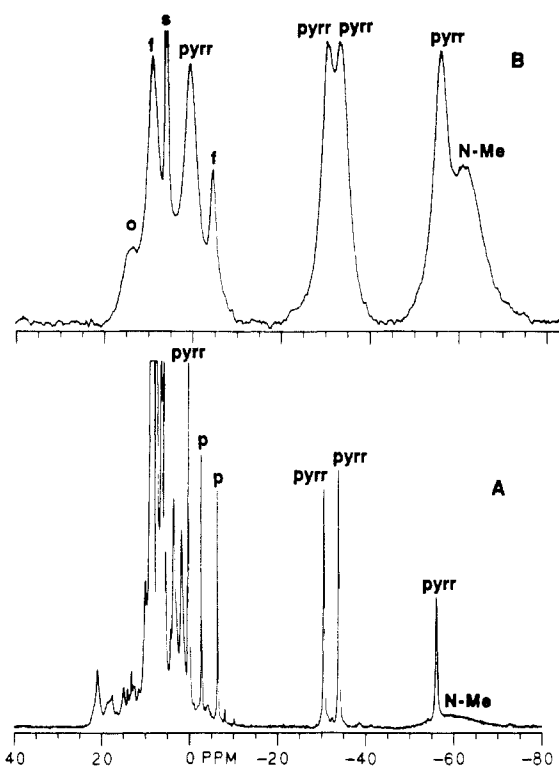


Figure 3. (A) 300-MHz ¹H NMR spectrum of [(*N*-MeTTP)Fe^{III}Cl]-[SbCl₆] and 2.6 equiv of [(Ph₃P)₂N][CN] in dichloromethane-*d*₂ solution at -90 °C. (B) 76.8-MHz ²H NMR spectrum of [(*N*-CD₃TTP-pyrrole-*d*₃)Fe^{III}Cl][SbCl₆] and 3 equiv of [(Ph₃P)₂N][CN] in dichloromethane at -90 °C. Resonance assignments follow those in Figure 2 with s (solvent), f (*N*-MeTTPH), o (TTPFe^{III}OFe^{III}TTP).

of [(*N*-CD₃TTP-pyrrole-*d*₃)Fe^{III}(5-MeIm)₂]²⁺ and [(*N*-CD₃TTP)Fe^{III}(5-MeIm)₂]²⁺ allows resonances at -38, -24, -11, and -0.3 ppm (as set out in Table II) to be assigned to the pyrrole protons, while a resonance at -17 ppm is assigned to the *N*-CD₃ group. Thus the upfield resonances in the ¹H NMR spectrum are due to pyrrole protons (the *N*-CH₃ resonance is too broad to be observed). Notice that two of these resonances in the ¹H NMR spectrum are split into doublets and the upfield pyrrole is broad, due to unresolved splitting. The two resonances at 26 and 33 ppm are assigned to the methyl resonances of 5-MeIm on the basis of their relative intensity and the absence of resonances in that region in comparable spectra obtained with imidazole. The low-spin 5-methylimidazole adduct can be observed at temperatures up to -50 °C, but the presence of traces of water in the imidazole results in hydrolysis to μ -oxo complexes on warming. The spectral features seen in trace B are also observed with samples containing less 4-methylimidazole. Consequently, these features cannot be caused by hydrogen bonding to the coordinated imidazole.

Trace A of Figure 3 shows the ¹H NMR spectrum of a dichloromethane solution of [(*N*-MeTTP)Fe^{III}Cl][SbCl₆] at -90

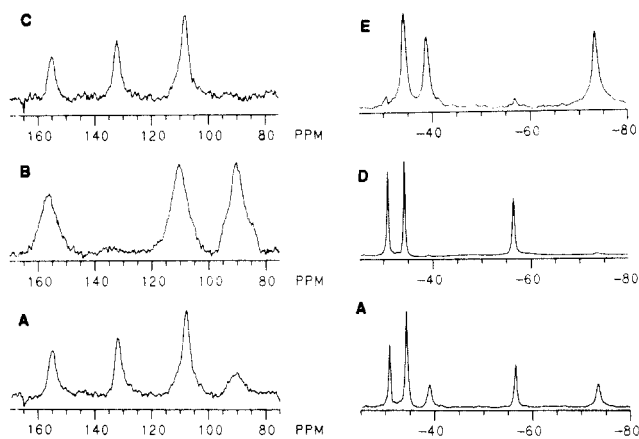
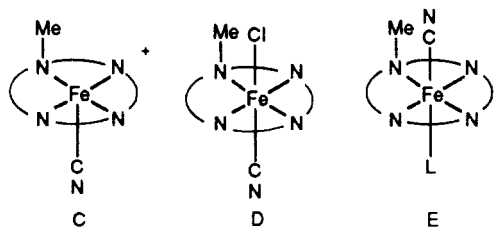


Figure 4. 300-MHz ^1H NMR spectrum of (A) $[(N\text{-MeTTP})\text{Fe}^{\text{III}}\text{Cl}]^+$ and 1.6 equiv of $[(\text{Ph}_3\text{P})_2\text{N}]\text{CN}$ in dichloromethane at -90°C , (B) $[(N\text{-MeTTP})\text{Fe}^{\text{III}}\text{Cl}]^+$ itself at -90°C , (C) high-spin $[(N\text{-MeTTP})\text{Fe}^{\text{III}}\text{CN}]$ obtained by subtraction of trace B from trace A, (D) $[(N\text{-MeTTP})\text{Fe}^{\text{III}}(\text{CN})_2]$ obtained with excess CN, and (E) the low-spin complex obtained by subtracting trace D from trace A. ^2H NMR spectroscopy on pyrrole- d_8 samples verifies the fact that all major resonances result from pyrrole protons.

$^\circ\text{C}$ in the presence of 2.6 equiv of $[(\text{Ph}_3\text{P})_2\text{N}][\text{CN}]$, a conveniently soluble source of cyanide ion. Trace B of Figure 3 shows the 76.8-MHz ^2H NMR spectrum of $[(N\text{-CD}_3\text{TTP}\text{-pyrrole-}d_8)\text{Fe}^{\text{III}}\text{Cl}][\text{SbCl}_6]$ in dichloromethane also in the presence of 3 equiv of cyanide ion. Four equally intense resonances due to the pyrrole deuterons are readily distinguished while the unique highest field resonance is assigned to the *N*-methyl group. The ^1H NMR spectrum in trace A shows the counterparts of these resonances and allows the resonances at -2 and -7 ppm to be assigned to the *p*-methyl protons of the *p*-tolyl groups on the basis of their absence in trace B and their relative intensity. Under the conditions utilized here, $[(N\text{-MeTTP})\text{Fe}^{\text{III}}(\text{CN})_2]$ is unstable. When warmed it is reduced, presumably by excess cyanide, back to an iron(II) *N*-methylporphyrin complex in a reaction that has also been observed for iron(III) porphyrins.¹⁷

At lower ratios of cyanide to iron, it is possible to detect two intermediates involved in cyanide addition. Trace A of Figure 4 shows the ^1H NMR spectrum obtained by adding 1.6 equiv of cyanide to a solution of $[(N\text{-MeTTP})\text{Fe}^{\text{III}}\text{Cl}][\text{SbCl}_6]$, while trace B shows the spectrum of $[(N\text{-MeTTP})\text{Fe}^{\text{III}}\text{Cl}]^+$ alone. In the downfield region new resonances appear that are indicative of the formation of a new, high-spin iron(III) complex. Inset C shows the difference spectrum obtained by subtracting the spectrum of the three pyrrole resonances for $[(N\text{-MeTTP})\text{Fe}^{\text{III}}\text{Cl}][\text{SbCl}_6]$ from the observed spectrum. Three resonances are clearly present in the 100–160-ppm region. Observations on the ^2H NMR spectrum of $[(N\text{-MeTTP})\text{-pyrrole-}d_8\text{-Fe}^{\text{III}}\text{Cl}]^+$ in the presence of cyanide confirm that these resonances are indeed due to pyrrole groups. These resonances are assigned to $[(N\text{-MeTTP})\text{Fe}^{\text{III}}\text{CN}]^+$ (structure C) by analogy to the chloro complex, $[(N\text{-MeTTP})\text{Fe}^{\text{III}}\text{Cl}]^+$. In the upfield region of Figure 4 there are also res-



onances due to two species, $[(N\text{-MeTTP})\text{Fe}^{\text{III}}(\text{CN})_2]$ and a second low-spin complex. Trace E shows a difference spectrum obtained by subtracting the spectrum of $[(N\text{-MeTTP})\text{Fe}^{\text{III}}(\text{CN})_2]$ (trace D) from trace A in Figure 4. Three equally intense resonances

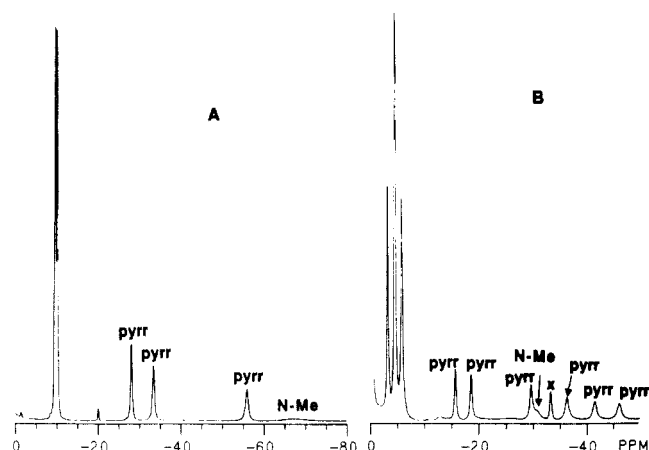


Figure 5. 300-MHz ^1H NMR spectra of $[(N\text{-MeTMP})\text{Fe}^{\text{III}}\text{Cl}][\text{SbCl}_6]$ in the presence of (A) 3 equiv of $[(\text{Ph}_3\text{P})_2\text{N}]\text{CN}$ in dichloromethane- d_2 at -90°C and (B) 13 equiv of Im in dichloromethane- d_2 at -90°C . Resonance X is due to the pyrrole protons of $(\text{TMP})\text{Fe}^{\text{III}}(\text{Im})_2^{2+}$. In both cases no resonances occur to low-field of 20 ppm. Resonance assignments follow those in Figures 2 and 3. In trace A the principal species is $[(N\text{-MeTMP})\text{Fe}^{\text{III}}(\text{CN})_2]$ and in B it is $[(N\text{-MeTMP})\text{Fe}^{\text{III}}(\text{Im})_2]^{2+}$.

are seen in the 0 to -80 ppm region. Observations made with the pyrrole- d_8 porphyrin confirm that these are pyrrole resonances. The general pattern is similar to that described above for $(N\text{-MeTTP})\text{Fe}^{\text{III}}(\text{CN})_2$, hence another low-spin species is present. This can have the six-coordinate structure D. However, we discount this in favor of structure E, a structure with the cyanide on the proximal side with the *N*-methyl group. Placing a ligand in this position will certainly pull the iron into the porphyrin plane, and this is likely to produce the high ligand field necessary to cause spin pairing. The opposite face, then, may be left vacant or it may be occupied by a chloride ligand. In contrast, structure D places the larger chloride ligand on the more crowded face of the porphyrin. Moreover, it is somewhat unlikely that addition of a weak-field ligand to such a position will cause spin pairing. Addition of more cyanide to the mixture of compounds seen in Trace A of Figure 4 results in their complete conversion into $(N\text{-MeTTP})\text{Fe}^{\text{III}}(\text{CN})_2$.

Trace A in Figure 5 shows the upfield portion of the 300-MHz ^1H NMR spectrum of a dichloromethane solution of $[(N\text{-MeTMP})\text{Fe}^{\text{III}}\text{Cl}][\text{SbCl}_6]$ in the presence of 2.7 equiv of cyanide at -90°C . Three pyrrole resonances and an *N*-methyl resonance are apparent along with two resonances due to the methyl groups of the mesityl substituents. Trace B of this figure shows the same complex in dichloromethane- d_2 at -90°C in the presence of 10 equiv of imidazole. The spectrum resembles that seen in trace B of Figure 2 except that there are no resonances in the 20–40-ppm region and the upfield region shows six, equally intense resonances that are assigned as pyrrole resonances as well as three resonances due to methyl groups of the mesityl substituents.

The spectral patterns seen in Figures 2–5 are those expected for low-spin ($S = 1/2$) iron(III) complexes of *N*-methylporphyrins. This conclusion is based on observations made for low-spin iron(III) porphyrin complexes^{18–20} and our previous demonstration of the similarities between the ^1H NMR spectra of metal complexes of porphyrins and *N*-alkylporphyrins in similar oxidation and spin states.^{5,6} These features include much narrower pyrrole resonances for the low-spin forms than for the high-spin forms and pyrrole resonances in the upfield region. For comparison the pyrrole resonance of $[\text{TTPFe}^{\text{III}}(\text{CN})_2]^-$ occurs at -42 ppm at -90°C and for $[\text{TTPFe}^{\text{III}}(5\text{-MeIm})_2]^+$ it occurs at -32 ppm at -90°C . These upfield shifts are consistent with ligand-to-metal spin-density transfer from π orbitals of the porphyrin into the d_{xz} or d_{yz} orbital of iron. For $[(N\text{-MeTTP})\text{Fe}^{\text{III}}(\text{CN})_2]$ there are four

(18) La Mar, G. N.; Del Guadio, J.; Frye, J. S. *Biochim. Biophys. Acta* 1977, 493, 422.

(19) La Mar, G. N.; Walker, F. A. *J. Am. Chem. Soc.* 1973, 95, 1782.

(20) Satterlee, J. D.; La Mar, G. N. *J. Am. Chem. Soc.* 1976, 98, 2804.

(17) Del Guadio, J.; La Mar, G. N. *J. Am. Chem. Soc.* 1976, 98, 3014.

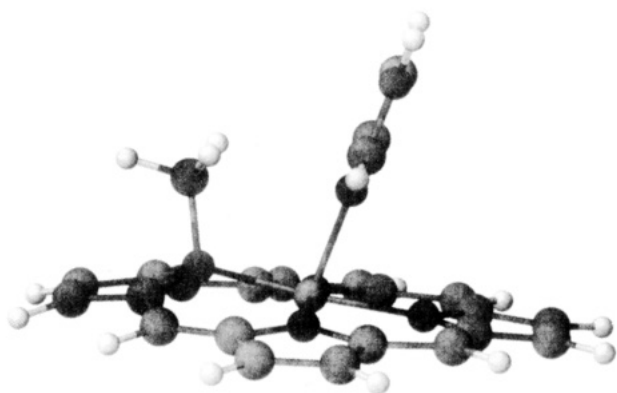


Figure 6. A computer-generated, energy-minimized plot showing the relative orientation of the *N*-methyl substituent and an imidazole ligand on the same side of the porphyrin plane. For clarity the imidazole ligand on the opposite side is not shown. Note that the imidazole ligand lies perpendicular to the Me–N–Fe–N axis.

pyrrole resonances as expected for a complex that retains the mirror symmetry that is intrinsic to *N*-methylporphyrins. For the imidazole complexes, however, additional splitting of the pyrrole resonances is seen. This must result from the orientation of one imidazole ligand and a lack of free rotation about its Fe–N bond. This situation pertains to the ligand that bonds to the iron on the same side of the porphyrin as the *N*-methyl group. That ligand cannot lie in the mirror plane of the *N*-methylporphyrin because such an orientation creates unfavorable contacts between the *N*-methyl group and the ligand. Most likely the imidazole ligand binds with its plane perpendicular to the mirror plane of the *N*-methylporphyrin and destroys the mirror symmetry. A view of a portion of the cation showing this relationship of the *N*-methyl substituent to an imidazole ligand, as obtained from an energy minimization calculation, is shown in Figure 6. As a consequence of the imidazole location, the eight pyrrole protons of the porphyrin are distinct and eight pyrrole resonances are expected. For $[(N\text{-MeTMP})\text{Fe}^{\text{III}}(\text{Im})_2]^{2+}$ six of these are apparent in Figure 5 while with $[(N\text{-MeTTP})\text{Fe}^{\text{III}}(5\text{-MeIm})_2]^{2+}$ five resonances (one broad resonance of intensity two) are seen (Figure 2). The remaining resonances must lie in the crowded region below -5 ppm, a fact that was confirmed by the ^2H NMR spectrum of $[(N\text{-CD}_3\text{TTP-pyrrole-}d_8)\text{Fe}^{\text{III}}(5\text{-MeIm})_2]^{2+}$.

The 5-methylimidazole resonance pattern is also consistent with our structural interpretation. The observation of two methyl resonances for $[(N\text{-MeTTP})\text{Fe}^{\text{III}}(5\text{-MeIm})_2]^{2+}$ and their intensity relative to the pyrrole resonances presents convincing evidence for the presence of two axial ligands. These are clearly distinct since one lies on the same side of the porphyrin plane as the *N*-methyl group while the other resides on the opposite side. The positions of these methyl resonances are entirely consistent with expectations based on the position of the corresponding resonance in low-spin $\text{PFe}^{\text{III}}(5\text{-MeIm})_2^+$.²⁰ The methyl resonance for $[\text{TPPFe}^{\text{III}}(5\text{-MeIm})_2]^+$ occurs at 23 ppm at -60 °C, i.e. in a position consistent with the methyl resonance of 5-MeIm seen in trace B of Figure 2.

Table II collects the spectral data seen for these new six-coordinate adducts and allows them to be compared to data gathered for other *N*-methylporphyrin complexes with a variety of metal ions. These six-coordinate adducts are the first examples in which all four pyrrole resonances of the *N*-alkylporphyrin appear upfield as expected for the previously described π contact shift mechanism.^{18–20} The position of the *N*-methyl resonance is also sensitive to the electronic structure. A rough estimate of the dipolar shift based on *p*-methyl resonance shifts and previously generated geometric factors²¹ leads to the conclusion that there is a large (100–300 ppm at -90 °C) upfield contact contribution for the *N*-Me group. The magnitude is similar to that seen for high-spin iron(III),⁸ iron(II),⁶ and nickel(II)²¹ complexes, but opposite in

sign. This sign reversal comes about because the $\sigma(d_{z^2-y^2})$ orbital is half-filled for the high-spin iron(III), iron(II), and nickel(II) cases, while it is empty for the low-spin iron(III) case.

There has been considerable interest in the ability of specific, fixed orientations of axial imidazole and pyridine ligands to break the inherent, 4-fold symmetry in synthetic porphyrins and to affect the electron distribution within the π -system of hemes.^{22–29} The observation of restricted rotation of the imidazole ligands in $[(N\text{-MeTTP})\text{Fe}^{\text{III}}(5\text{-MeIm})_2]^{2+}$ and $[(N\text{-MeTMP})\text{Fe}^{\text{III}}(5\text{-MeIm})_2]^{2+}$ represents a novel case in which a nontethered ligand is capable of producing a distinctly lower symmetry that has defined spectroscopic consequences on the porphyrin.²⁹ The magnitude of the splitting of the pyrrole protons that are produced, at least at -90 °C, is quite large. A previous study of the reaction of imidazole with $(N\text{-MeTTP})\text{Fe}^{\text{II}}\text{Cl}$ indicated that the added base replaced a chloride ligand.⁶ The resulting adducts, which were formed under conditions analogous to those used here, retained the spectral features of five-coordinate, high-spin ($S = 2$) species. In particular, there was no evidence for further splitting of the four pyrrole resonances so that the imidazole ligand coordinated on the open face of the *N*-methyl porphyrin remains free to rotate about the Fe–N bond.

The results described here serve to establish for the first time the ability of an *N*-methylporphyrin ligand to accommodate six-coordination by the central metal. Initial work on *N*-methylporphyrins emphasized the steric protection of the metal that the *N*-methyl substituent provided and demonstrated their ability to stabilize five-coordinate structures for a variety of metal ions.^{4,30,31} Recent work by Mansuy and co-workers has shown that six-coordinate structures can form in the *N*-substituted and *N,N*-disubstituted porphyrins where the *N*-substituent(s) contain functional groups that are also capable of attaching themselves to the metal.³²

In conclusion, this work broadens our understanding of the coordination of iron in a *N*-methylporphyrin environment and serves to further establish the similarities of porphyrin and *N*-methylporphyrin complexes. Both form high-spin ($S = 5/2$), five-coordinate iron(III) complexes, both form μ -oxo-bridged iron(III) dimers, and both form low-spin ($S = 1/2$), six-coordinate iron(III) complexes with strong field axial ligands (cyanide, imidazoles). Within each of these pairs there is considerable analogy in magnetic and NMR spectral properties despite the inherent lower symmetry of the *N*-substituted porphyrins. There are also parallels that can be drawn between the *N*-substituted porphyrins and the thiaporphyrin ligands.³³ Both have similar symmetry and both coordinate metal ions so that the unique, five-membered-ring component (*N*-substituted pyrrole or thiophene) is bent out of the plane of the remaining three pyrrole rings. Similarities between high-spin, five-coordinate iron(III) complexes of *N*-methylporphyrins and thiaporphyrins have been previously noted. Although six-coordinate iron thiaporphyrin complexes analogous to $[(N\text{-MeTTP})\text{Fe}^{\text{III}}(\text{Im})_2]^{+2}$ have yet to be made, a six-coordinate

(22) Traylor, T. G.; Berzins, A. P. *J. Am. Chem. Soc.* **1980**, *102*, 2844.

(23) Goff, H. *J. Am. Chem. Soc.* **1980**, *102*, 3252.

(24) Walker, F. A. *J. Am. Chem. Soc.* **1980**, *102*, 3254.

(25) Walker, F. A.; Buehler, J.; West, J. T.; Hinds, J. L. *J. Am. Chem. Soc.* **1983**, *105*, 6923.

(26) Walker, F. A.; Balke, V. L.; McDermott, G. A. *J. Am. Chem. Soc.* **1982**, *104*, 1569.

(27) Latos-Grażyński, L. *Biochimie* **1983**, *65*, 143.

(28) Momenteau, M.; Mispelter, J.; Loock, B.; Lhoste, J.-M. *J. Chem. Soc., Perkin Trans.* **1985**, 221.

(29) Nakamura, M.; Grooves, J. T. *Tetrahedron* **1988**, *44*, 3225. This reports hindered 2-methylimidazole rotation in $[\text{TMPFe}^{\text{III}}(2\text{-MeIm})_2]^+$, but the less sterically encumbered $[\text{TMPFe}^{\text{III}}(N\text{-MeIm})_2]^+$ and $[\text{TPPFe}^{\text{III}}(2\text{-MeIm})_2]^+$ do not show this effect. Since the present work shows effects of hindered rotation with imidazoles smaller than 2-MeIm and with TPP derivatives, the origin of the rotational barrier must be different.

(30) Anderson, O. P.; Lavalley, D. K. *J. Am. Chem. Soc.* **1976**, *98*, 4670.

(31) Anderson, O. P.; Lavalley, D. K. *J. Am. Chem. Soc.* **1977**, *99*, 1404.

(32) Battioni, J.-P.; Artaud, I.; Dupré, D.; Leduc, P.; Akhrem, I.; Mansuy, D.; Fischer, J.; Weiss, R.; Morgenstern-Badarau, I. *J. Am. Chem. Soc.* **1986**, *108*, 5598.

(33) Latos-Grażyński, L.; Lisowski, J.; Olmstead, M. M.; Balch, A. L. *Inorg. Chem.* **1989**, *28*, 1183.

(21) Latos-Grażyński, L. *Inorg. Chem.* **1985**, *24*, 1681.

thiaporphyrin complex of rhodium(III) with two axial chloride ligands has been thoroughly characterized.³⁴

Experimental Section

Materials. TTPH₂,³⁵ pyrrole-*d*₃-TTPH₂,³⁶ and TMPH₂³⁷ were prepared by reported procedures.

Preparation of Compounds. Diphenylmethylsulfonium Tetrafluoroborate. A mixture of 0.5 mL (3.0 mmol) of diphenyl sulfide, 0.95 mL (1.52 mmol) of iodomethane, and 5 mL of nitromethane was placed in a 25-mL flask and 0.7 g (3.6 mmol) of silver tetrafluoroborate was added. The reaction slurry was stirred for 1 h. The yellow solid was removed by filtration through Celite, and the filtrate was evaporated with use of a rotary evaporator. The resulting pale yellow oil was stirred with diethyl ether overnight to yield a white powder. The powder was collected on a Büchner funnel and dried under vacuum. Yield: 0.62 g (71% based on diphenyl sulfide). The solid can be stored in a desiccator for months. ¹H NMR (CDCl₃) δ 3.6 (s), 7.6 (m), 7.9 ppm (d). The methyl-deuterated compound, [CD₃SPh₂]⁺BF₄⁻, was prepared in the same manner with methyl-*d*₃ iodide.

***N*-Methyltetramesitylporphyrin.** Tetramesitylporphyrin, 0.124 g (0.16 mmol), was dissolved in 100 mL of *o*-dichlorobenzene and warmed to 140 °C. Solid [Ph₂SMe]⁺BF₄⁻ (0.228 g, 0.79 mmol) was added. The solution was stirred at 140 °C for 12 h. The progress of the reaction was monitored by observing its absorption spectrum. Upon disappearance of the Soret band (416 nm) of the starting material, the solution was cooled and washed with 100 mL of concentrated ammonium hydroxide. The volume of the organic phase was reduced on the rotary evaporator at 100 °C, and the sample was subjected to chromatography on a 5 cm × 15 cm column of basic alumina. TMPH₂ was eluted with methylene chloride. *N*-MeTMPH was eluted with 5% ethyl acetate in toluene. *N*-MeTMP can be eluted with 10% ethyl acetate/toluene. The *N*-MeTMPH solution was evaporated to dryness and further dried under vacuum; yield, 0.11 g, 91%. The reaction appears to be stoichiometric in that only a slight excess of methylating agent (1.2 equiv) is required for complete reaction. The reaction temperature of 140 °C is critical. At lower temperatures, methylation is very slow, while at higher temperature (150 °C) the amount of dimethylated products increases significantly. Nonchlorinated solvents such as *o*-xylene (bp 144 °C) do not work for this reaction. ¹H NMR (CD₂Cl₂) δ (ppm), *N*-Me, -3.73 ppm (s); *N*-H, -1.90 (s), *o*-CH₃, 1.59 (s), 1.69 (s), 2.08 (s), 2.31 (s); *p*-CH₃, 2.59 (s); pyrrole-H, 8.53 (s), 8.34 (d, *J* = 4.3 Hz), 8.22 (d, *J* = 4.3 Hz), 7.52 (s); *m*-H, 7.33 (s), 7.30 (s), 7.22 (s, twice the intensity of the other *m*-H resonances); UV-vis (CH₂Cl₂) λ_{max} (ε × 10⁴ cm⁻¹ M⁻¹) 428 (24.69), 524 (1.709), 560 (1.422), 614 (0.8058), 674 nm (0.7297).

Iron(II) Insertion into *N*-Methylporphyrins. Iron(II) chloride was prepared by heating 0.076 g (0.47 mmol, 1.5 equiv) of anhydrous iron(III) chloride and excess (ca. 1 g) iron powder in 1,2-dimethoxyethane (distilled from sodium under N₂) under N₂ until the solution became colorless (from brown, usually <3 h). To the iron(II) solution was added 0.25 g (0.31 mmol) of *N*-MeTMPH as a powder. The solution immediately became deep green and heating was discontinued. An aliquot of 0.1 mL of 2,2,6,6-tetramethylpiperidine was added. The solution was then filtered through Celite and dried on the rotary evaporator. The residue was repeatedly redissolved in a minimum of benzene, filtered, and dried under vacuum until no residue from metal salts remained in the flask. This material was pure enough for most applications. The compound could be recrystallized from benzene/isooctane; yield, 0.21 g, 76%; UV-vis (CDCl₃) λ_{max} (ε × 10⁴ cm⁻¹ M⁻¹) 448 (19.067), 460 (16.258), 570 (1.715), 616 (2.056), 664 nm (1.470).

(Thian⁺)SbCl₆. Thianthrene (0.5 g, 2 mmol) was dissolved in 15 mL of methylene chloride. A solution of 0.37 mL (2 mmol) of antimony pentachloride was added and a purple solid precipitated immediately. It was collected by filtration under N₂ and dried under vacuum. The solid is stable in a desiccator for months.

Oxidation of (*N*-MeTMP)Fe^{II}Cl. (*N*-MeTMP)Fe^{II}Cl (0.050 g, 0.056 mmol) was dissolved in 50 mL of benzene (purged with N₂ for 15 min) and 0.047 g (0.085 mmol, 1.5 equiv) of [Thian⁺][SbCl₆]⁻ was added as powder. The solution was stirred for 30 min and then the solvent was removed on a rotary evaporator.

X-ray Crystallographic Studies. A suitable crystal of [(*N*-MeTTP)-Fe^{III}Cl][SbCl₆].1.5(toluene) was obtained by slow diffusion of hexane into a saturated toluene solution of the complex with use of a crystal

Table III. Crystal Data, Data Collection, and Structure Solution Parameters for [(*N*-MeTTP)Fe^{III}Cl][SbCl₆].1.5(toluene)

formula	C _{59.5} H ₅₁ Cl ₇ FeN ₄ Sb
fw	1247.86
color and habit	deep purple block
crystal system	triclinic
space group	P1
<i>a</i> , Å	13.170 (6)
<i>b</i> , Å	14.591 (10)
<i>c</i> , Å	15.702 (14)
α, deg	83.78 (7)
β, deg	79.82 (6)
γ, deg	74.34 (5)
<i>V</i> , Å ³	2853 (4)
<i>T</i> , K	130
<i>Z</i>	2
cryst dimens, mm	0.14 × 0.20 × 0.33
<i>d</i> _{calc} , g cm ⁻³	1.45
radiation, Å	MoKα (λ = 0.71069)
μ(MoKα), cm ⁻¹	11.0
range of transmission factors	0.81–0.88
diffractometer	P2 ₁ , graphite monochromator
scan method	ω, 1.1° range, 1.3° offset for bkgnd
scan speed, deg min ⁻¹	10
2θ range, deg	0–45°
octants collected	<i>h</i> , ± <i>k</i> , ± <i>l</i>
no. of data collected	7463
no. of unique data	7463
no. of data used in refinement	4842 [<i>I</i> > 2σ(<i>I</i>)]
no. of parameters refined	375
<i>R</i> ^a	0.069
<i>R</i> _w ^a	0.069 [<i>w</i> = 1/σ ² (<i>F</i> _o)]

$$^a R = \sum ||F_o| - |F_c|| / |F_o| \text{ and } R_w = \sum ||F_o| - |F_c|| w^{1/2} / \sum |F_o w^{1/2}|.$$

growing tube with a constriction at the interface of the two solutions.³⁸ A crystal was mounted on a glass fiber with silicone grease and positioned in the cold stream of the X-ray diffractometer. Only random fluctuations (<2%) in the intensities of two standard reflections were observed during the course of data collection. Crystal data are given in Table III.

The usual corrections for Lorentz and polarization effects were applied to the data. Crystallographic programs used were those of SHELXTL, version 5, installed on a Data General Eclipse computer. Scattering factors and corrections for anomalous dispersion were from the *International Tables*.³⁹ The structure was solved by direct methods. The solid consists of one [(*N*-MeTTP)Fe^{III}Cl]⁺, two half-ions of SbCl₆⁻ situated on centers of symmetry, one-half of a toluene packed around a center of symmetry, and a full molecule of toluene which is in turn disordered into two equal but slightly rotated molecules. The latter rings were refined as rigid groups. There also is disorder in the chlorine atoms of one of the SbCl₆⁻ groups. It was modeled by the assignment of two equally probable positions for two of the chlorine atoms.

Hydrogen atoms were included at calculated positions with use of a riding model, with C–H of 0.96 Å and *U*_H = 1.2*U*_C. Those hydrogens of the carbons of the toluenes of crystallization were omitted. An absorption correction was applied.⁴⁰ Final refinement was carried out with anisotropic thermal parameters for Fe, Sb, and Cl. The largest feature on a final difference map was 1.27 e Å⁻³ in height and was in the vicinity of the disordered SbCl₆⁻ group. The largest shift/esd in the final cycle of refinement was 0.007 for rotation of the methyl group of C(49).

Formation of Low-Spin Complexes. To the appropriate solution of iron(III) *N*-methylporphyrin in methylene chloride at -90 °C was added, by titration, a 0.3 to 0.5 M solution of the appropriate ligand in methylene chloride. The cyanide source was bis(triphenylphosphino)iminium cyanide. Imidazole was recrystallized from benzene. 4-Methylimidazole was used as received from Aldrich.

Instrumentation. NMR spectra were recorded on Nicolet NT-360 and NT-500 and GE QE-300 spectrometers operating in the quadrature mode (¹H frequencies are 360, 500, and 300 MHz, respectively). The spectra were collected over a 40-kHz bandwidth with 16 K data points and a 6-μs 90° pulse. For a typical paramagnetic spectrum, between 500 and 2000

(34) Latos-Grażyński, I.; Lisowski, J.; Olmstead, M. M.; Balch, A. L. *Inorg. Chem.* **1989**, *28*, 3328.

(35) Adler, A. D.; Longo, F. R.; Karplus, F.; Kim, J. J. *Inorg. Nucl. Chem.* **1970**, *32*, 2443.

(36) Boersma, A. D.; Goff, H. M. *Inorg. Chem.* **1982**, *21*, 581.

(37) Lindsay, J. S.; Hsu, H. C.; Schreiman, I. C. *Tetrahedron Lett.* **1986**, 4969.

(38) Balch, A. L.; Chan, Y. W.; Olmstead, M. M. *J. Am. Chem. Soc.* **1985**, *107*, 6510.

(39) *International Tables for X-ray Crystallography*; Kynoch Press: Birmingham, England, 1974; Vol. IX.

(40) The absorption correction is made with use of program XABS, H. Hope and B. Moezzi. The program obtains an absorption tensor for *F*_o - *F*_c differences. Moezzi, B. Ph.D. Dissertation, University of California, Davis, 1987.

transients were accumulated with a delay time of 50 ms. The signal-to-noise ratio was improved by apodization of the free induction decay. The residual proton peak of dichloromethane- d_2 was used as a secondary reference (5.32 ppm). Intense diamagnetic resonances arising from $[(\text{PPh}_3)_2\text{N}]\text{CN}$ and 4-Melm were suppressed with a Super WEFT pulse sequence.⁴¹ This resulted in inversion of some slowly relaxing diamagnetic resonances. The delay time τ between the 180° pulse and the 90° pulse was typically greater than 50 ms, and the effect on the intensity of the paramagnetic resonances was negligible. Figure 6 was obtained with the CAChe system of Tektronix Inc.

Acknowledgment. We thank the National Institutes of Health (Grant GM-26226) for support and Dr. Linda M. Hirschy of Tektronix, Inc. for generating Figure 6 using the CAChe molecular modeling program.

(41) Inubushi, T.; Becker, E. D. *J. Magn. Reson.* 1983, 51, 128-133.

Registry No. $[\text{Ph}_2\text{SMe}]\text{BF}_4$, 10504-60-6; $(N\text{-MeTMP})\text{Fe}^{\text{II}}\text{Cl}$, 128901-96-2; $(\text{Thian}^+)\text{SbCl}_6$, 76598-11-3; $[(N\text{-MeTPP})\text{Fe}^{\text{III}}\text{Cl}][\text{SbCl}_6] \cdot 1.5(\text{toluene})$, 128901-98-4; $N\text{-MeTTPFe}^{\text{II}}\text{Cl}$, 95675-71-1; $(N\text{-MeTTP})\text{Fe}^{\text{III}}(\text{CN})_2$, 128901-99-5; $[(N\text{-MeTTP})\text{Fe}^{\text{III}}(5\text{-MeIm})_2]^{2+}$, 128901-95-1; $[(N\text{-MeTMP})\text{Fe}^{\text{III}}\text{Im}_2]^{2+}$, 128901-94-0; $[(N\text{-MeTMP})\text{Fe}^{\text{III}}\text{Cl}]^+$, 128902-00-1; $[(N\text{-MeTTP})\text{Fe}^{\text{III}}\text{Cl}][\text{SbCl}_6]$, 128902-01-2; N -methyltetramesitylporphyrin, 128901-93-9; tetramesitylporphyrin, 56396-12-4; iodomethane, 74-88-4; diphenyl sulfide, 139-66-2; silver tetrafluoroborate, 14104-20-2; thianthrene, 92-85-3; antimony pentachloride, 7647-18-9.

Supplementary Material Available: Tables of atomic coordinates, bond distances, bond angles, anisotropic thermal parameters, hydrogen atom positions, and crystal refinement data for $[(N\text{-MeTTP})\text{FeCl}][\text{SbCl}_6] \cdot 1.5(\text{toluene})$ (8 pages); listings of observed and calculated structure factors (29 pages). Ordering information is given on any current masthead page.

Reactions Involving Chelate Ring Opening or Metal Ion Relocation in the Formation of Luminescent Complexes Containing both Gold and Iridium

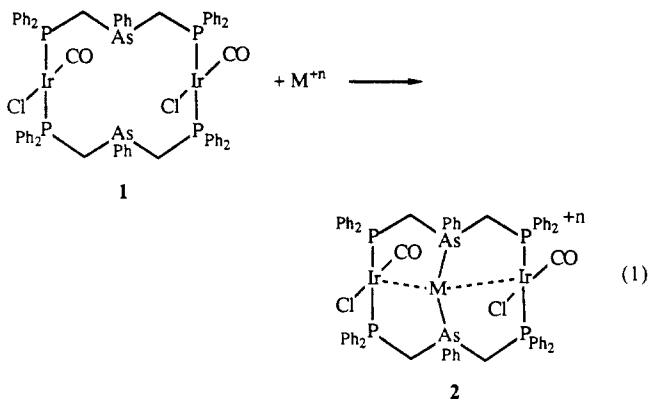
Alan L. Balch,* Vincent J. Catalano, Bruce C. Noll, and Marilyn M. Olmstead

Contribution from the Department of Chemistry, University of California, Davis, California 95616. Received March 19, 1990

Abstract: Treatment of $\text{Ir}(\text{CO})_2\text{Cl}$ (p -toluidine) with 2 equiv of dpmp (bis(diphenylphosphinomethyl)phenylphosphine) and ammonium hexafluorophosphate yields ivory $[\text{Ir}(\text{dpmp})_2\text{CO}][\text{PF}_6]$, **5**, which an X-ray crystal structure shows to have a five-coordinate geometry with one six-membered and one four-membered chelate ring. This structure is compared with that of $[\text{Ir}(\text{dpma})_2\text{CO}][\text{PF}_6]$, **3** (dpma is bis(diphenylphosphinomethyl)phenylarsine), which is trigonal-bipyramidal with two six-membered chelate rings that span axial and equatorial coordination sites. Addition of 3 equivs of Me_2SAuCl to **5** results in the formation of orange $[\text{Ir}(\text{CO})\text{ClAu}(\text{AuCl})_2(\mu\text{-dpmp})_2][\text{PF}_6]$, **6**, which has a planar $\text{Ir}(\text{CO})\text{Cl}(\text{P})_2$ unit connected to the trans, terminal phosphorus atoms of the dpmp ligands, an Au(I) ion bound to the two internal phosphorus atoms, and AuCl moieties attached to the remaining two terminal phosphorus atoms of the dpmp ligands. Complex **6** has a strong absorption at 454 nm and photoemissions at 568 and 660 nm. Treatment of **6** with KCN or **5** with KCN and Me_2SAuCl results in the formation of centrosymmetric $[\text{Au}_2\text{Ir}(\text{CN})_2(\mu\text{-dpmp})_2][\text{PF}_6]$, **7**, with a linear Au-Ir-Au chain. The conversion of **6** to **7** results not only in loss of a gold ion but also extensive rearrangement at the core to go from a T-shaped Au_2AuIr unit to a linear AuIrAu section. Complex **7** is intensely magenta ($\lambda_{\text{max}}(\text{absorption}) = 578 \text{ nm}$) with photoemission at 612 and 782 nm.

Introduction

The metallomacrocyclic **1** and its rhodium analogue have been useful starting materials for the rational preparation of a wide variety of heterotrinnuclear complexes via reaction 1.¹ Both



transition-metal ions (including Cu(I), Ag(I), Au(I), Pd(II),

Rh(I), and Ir(I))² and main-group ions (including Tl(I), In(I), Sn(II), and Pb(II))³ have been incorporated into the framework provided by **1**. We have also recently discovered another route to the formation of mixed-metal trinuclear species. This involves the opening of six-membered chelate rings in the complex $[\text{Ir}(\text{dpma})_2(\text{CO})][\text{PF}_6]$, **3** (dpma is bis(diphenylphosphinomethyl)phenylarsine, the same ligand seen in eq 1).⁴ In this process, reaction 2, there is considerably more bond breaking than necessary in reaction 1. In fact, only the Ir-CO bond is retained (as is the 2:1:1 dpma:Ir:CO stoichiometry). Eight metal-ligand bonds must break in the process, while seven new metal-ligand bonds as well as two gold-iridium bonds are formed. This opening of the six-membered chelate ring in **3** was particularly surprising,

(2) (a) Balch, A. L.; Fossett, L. A.; Olmstead, M. M.; Oram, D. E.; Reedy, P. E., Jr. *J. Am. Chem. Soc.* 1985, 107, 5272. (b) Balch, A. L.; Fossett, L. A.; Olmstead, M. M.; Reedy, P. E., Jr. *Organometallics* 1986, 5, 1929. (c) Balch, A. L.; Olmstead, M. M.; Neve, F.; Ghedini, M. *New J. Chem.* 1988, 12, 529, and references in each.

(3) (a) Balch, A. L.; Nagle, J. K.; Olmstead, M. M.; Reedy, P. E., Jr. *J. Am. Chem. Soc.* 1987, 109, 4123. (b) Balch, A. L.; Olmstead, M. M.; Oram, D. E.; Reedy, P. E., Jr.; Reimer, S. H. *J. Am. Chem. Soc.* 1989, 111, 4021.

(4) Balch, A. L.; Catalano, V. J.; Olmstead, M. M. *J. Am. Chem. Soc.* 1990, 112, 2010.

(1) Balch, A. L. *Pure Appl. Chem.* 1988, 60, 555.